In Situ Re-endothelialization *via* Multifunctional Nanoscaffolds

Lee-Chun Su,[†] Hao Xu,[‡] Richard T. Tran,[§] Yi-Ting Tsai,[†] Liping Tang,[†] Subhash Banerjee,[‡] Jian Yang,[*,§] and Kytai T. Nguyen[*,†]

[†]Department of Bioengineering, University of Texas at Arlington, Arlington, Texas 76010, United States, [‡]Department of Internal Medicine, University of Texas Southwestern Medical Center at Dallas, Dallas, Texas 75390, United States, and [§]Department of Biomedical Engineering, Materials Research Institute, The Huck Institutes of The Life Sciences, The Pennsylvania State University, University Park, Pennsylvania 16802, United States

ABSTRACT The endothelium monolayer lining in the luminal side of blood vessels provides critical antithrombotic functions. Damage to these cells will expose a highly thrombogenic subendothelium, which leads to pathological vascular changes. Using combined tissue engineering and ligand−receptor targeting strategy, we developed a biodegradable urethane-doped polyester (UPE) multifunctional targeting nanoparticle (MTN) scaffold system with dual ligands: (1) glycoprotein 1b (GP1b) to target the injured arterial endothelium and subendothelium and (2) anti-CD34 antibodies to capture endothelial progenitor cells for endothelium regeneration. The fabricated spherical MTNs of 400 nm were found to be cytocompatible and hemocompatible. Both the *in vitro* and *ex vivo* targeting of these nanoscaffolds not only showed binding specificity of MTNs onto the von Willebrand factor -coated surfaces that simulate the injured arterial walls but also competed with platelets for binding onto these injured sites. Further *in vivo* study has revealed that a single delivery of MTNs upon vascular injury reduced neointimal hyperplasia by 57% while increased endothelium regeneration by ~60% in 21 days. These results support the promise of using MTN nanoscaffolds for treating vascular injury *in situ*.

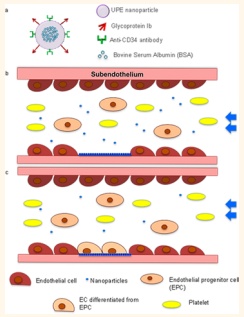

KEYWORDS: multifunctional nanoscaffolds · endothelium regeneration · vascular injury · vascular targeting · urethane-doped polyester (UPE)

Percutaneous transluminal coronary angioplasty (PTCA) and stenting have been the central therapies to relieve arterial obstruction. Unfortunately, these surgical procedures are also known to damage vascular endothelium and cause inflammation.[1,2] In physiological conditions, healthy endothelium produces various vasoactive molecules, which regulate arterial reactivity and maintain normal homeostasis.[3] Vascular injury caused by PTCA provokes prothrombogenic reactions in the form of von Willebrand factor (vWF) and P-selectin overexpression on the damaged endothelium and subendothelium layer, which subsequently triggers platelet adhesion, aggregation, and activation, along with smooth muscle cell proliferation.[4] These pathogenic processes eventually lead to restenosis, which considerably limits the long-term efficacy of these interventions.[5]

Several approaches, including drug-eluting stents (DES), have been developed to reduce restenosis by releasing antimitotic agents to local vascular tissues.[6] However, drugs released from DES can also delay endothelial regeneration and contribute to an increased rate of late-stent thrombosis.[7] Since Asahara *et al*. first discovered CD34(+) KDR(+) endothelial progenitor cells (EPCs) in 1997,[8] several therapeutic approaches using EPCs to regenerate endothelium have been investigated.[9] For example, capturing EPCs *in situ via* the coating of anti-CD34 antibodies on vascular grafts or stents has been reported with promising results to demonstrate the feasibility of an EPC-capturing strategy.[10,11] Yet enhancing EPC homing to the damaged areas of arteries through a minimally invasive method remains a challenge for vascular endothelialization.

In this study, we developed platelet-mimicking and EPC-capturing nanoparticles (NPs) to target injured blood vessels and encourage endothelium regeneration (Figure 1a). Urethane-doped polyesters (UPEs), citrate-based, biodegradable, and hemocompatible elastomers developed in our laboratory, were chosen for NP material. UPEs have shown great potential in multiple tissue engineering applications including vascular tissue engineering.[12,13] In addition to their excellent cytocompatibility and hemocompatibility, UPEs possess many carboxyl

* Address correspondence to (K. T. Nguyen) knguyen@uta.edu; (J. Yang) jxy30@psu.edu.

Received for review August 18, 2014 and accepted September 11, 2014.

Published online September 15, 2014
10.1021/nn504636n

and hydroxyl units, thus providing rich chemical functionalities for biomolecule conjugation, which is essential for surface modification of the NPs. In this study, glycoprotein Ib (GPIb) and anti-CD34 antibodies were conjugated on the NPs to make the multifunctional targeting nanoparticles (MTNs) (Figure 1a−c). Conjugation of GPIb enables the NPs to target vWF and P-selectin, which are overexpressed and/or deposited on the injured arterial wall,[14] whereas anti-CD34 antibodies conjugated on the NPs are used for capturing EPCs from the circulation once the NPs are anchored on the injured arterial wall.[15] Previous studies demonstrated that the hydrodynamic dislodging forces exerted on the NPs adhering on the vessel wall are less than that on platelets and leukocytes, which are at micrometer sizes.[16] Thus, MTNs might be easier than platelets to adhere on the injured blood vessel and prohibit subsequent platelet adhesion and thrombosis. In addition to competing with the platelets, MTNs might act as a scaffold to capture circulating EPCs for regenerating endothelium *in situ*. To test these hypotheses, a series of studies were carried out to investigate several pivotal aspects of the design: (1) targeting specificity to vascular injury; (2) competitive binding with platelets; (3) *in situ* EPC capturing in the bloodstream; and (4) efficacy on regeneration of endothelium *in vivo*.

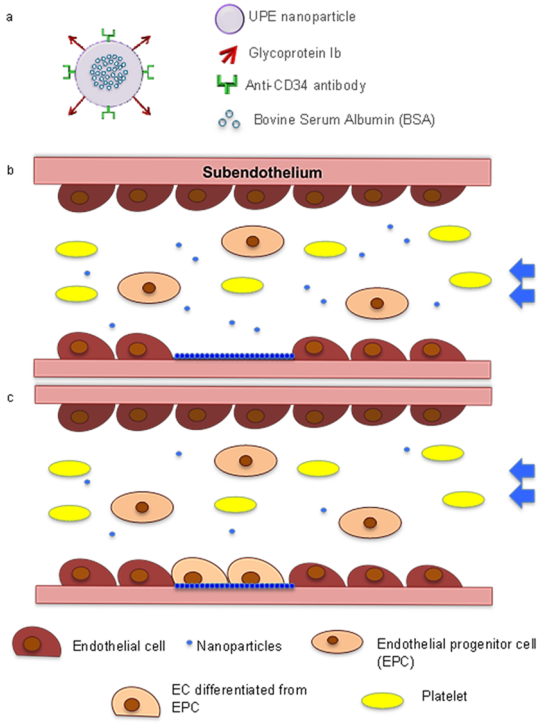

Figure 1. Schematics of the multitargeting nanoparticles (MTNs). (a) Design of MTNs. BSA was loaded as the protein model in UPE nanoparticles (for future animal studies, BSA will be replaced with growth factors such as VEGF). (b) Nanoparticle targeting to injured endothelium. (c) Re-endothelization is prompted by platelet mimicking, EPC-capturing MTN scaffolds.

RESULTS

Particle Fabrication and Characterization. Scanning electron microscopy (SEM) and transmission electron microscopy (TEM) showed that fabricated NPs were spherical with smooth surfaces (Figures 2a,b). Conjugation of GP1b and anti-CD34 antibodies slightly increased the particle sizes from 420 to 450 nm in diameter (Table 1). BSA loading efficiency in the UPE NPs was about 65%. As shown in Figure 2c, 40% of loaded BSA was quickly released within the first day of study followed by a sustained release up to 21 days (~2% /day). Particles degraded with a higher rate within the initial 15 days and then slowed for the remaining time. After 30 days, particles were degraded about 90%.

***In Vitro* Hemocompatibility and Cytocompatibility of MTNs.** Hemocompatibility of MTNs was evaluated by examining the adhesion and activation of platelets on an MTN-coated surface. The amount of platelets adhered on an MTN-coated surface was significantly less (p = 0.02) compared to that adhered on a vWF-coated surface (Figure 3a). The percentage of activated platelets (CD62p(+) or PAC-1(+)) was also significantly lower on MTN-coated surfaces compared to that on vWF-coated surfaces (Figure 3b). SEM showed that most platelets that adhered on vWF-coated surfaces were deformed and extensively aggregated (Figure 3.c1), another indication of platelet activation. On the

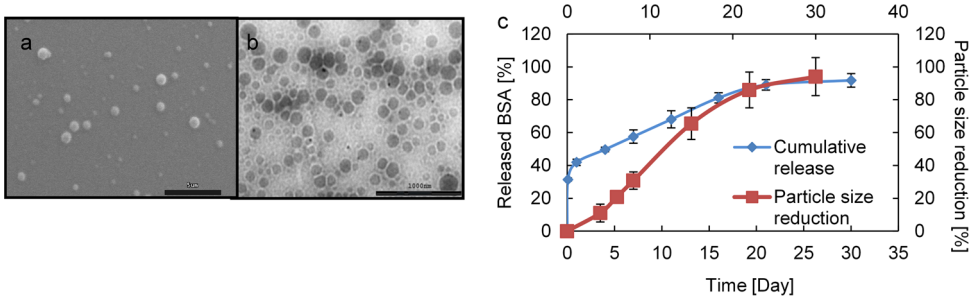

Figure 2. Characterization of the MTN nanoparticles. (a) SEM image; (b) TEM image; (c) cumulative release curve of bovine serum albumin from the nanoparticle and particle size reduction rate (degradation rate) of the nanoparticle over time when incubated in PBS at 37 °C. N = 3.

MTN-coated surface, fewer platelets were found adhered (highlighted in the red circle) with less platelet aggregation and deformation (Figure 3.c2). *In vitro* cytotoxicity was evaluated by incubating human aortic endothelial cells (HAECs) with MTNs at various concentrations. We find no apparent cell toxicity of MTNs to HAECs for up to 100 μg/mL. From 200 to 1000 μg/mL, there are slight decreases in cell viability as the NP concentrations increased, yet the cell viability is above 90% for all samples (Figure 3d). These results demonstrate that our MTNs are cytocompatible with HAECs.

MTN's Targeting to vWF *in Vitro* and Injured Blood Vessels *ex Vivo*. Under 10 dyn/cm^2 flow, more MTNs (Figure 4.a2) than the unmodified (control) NPs (Figure 4a1) were immobilized on vWF-coated surfaces. Approximately 93% and 42% of vWF-coated surfaces were occupied by MTNs under static and dynamic conditions, respectively, whereas only 5% and 3% of the vWF-coated surfaces were covered by the control NPs (Figure 4a3). These results support that MTNs have higher specificity to surface vWF than control NPs.

In the ex *vivo* targeting study, MTNs were also found to cover a much bigger areas of the injured arteries with high density of the particles (indicated by higher fluorescent intensity) compared to the control NPs (Figure 4b1). The amount of MTNs nearly doubled compared to that of the control NPs (Figure 4b2).

Binding Competition of MTNs with Platelets. The ability of MTNs to compete with platelets for the injured endothelium was also tested *in vitro.* In support of our hypothesis, we observed that the presence of MTNs reduced by ~50% platelet adherence to the vWF-coated surface compared with that of the controls (Figure 5a). SEM images confirmed that the vWF-coated surface was covered with platelet aggregations when only platelets were incubated without MTNs

TABLE 1. Size, Polydispersity, and Surface Charge of UPE Nanoparticles Measured by DLS before and after Surface Modification

sample	D_{av} [nm]	polydispersity [PD]	zeta potential [mV]
control NPs	420	0.335	−47.0
MTNs	450	0.357	−49.0

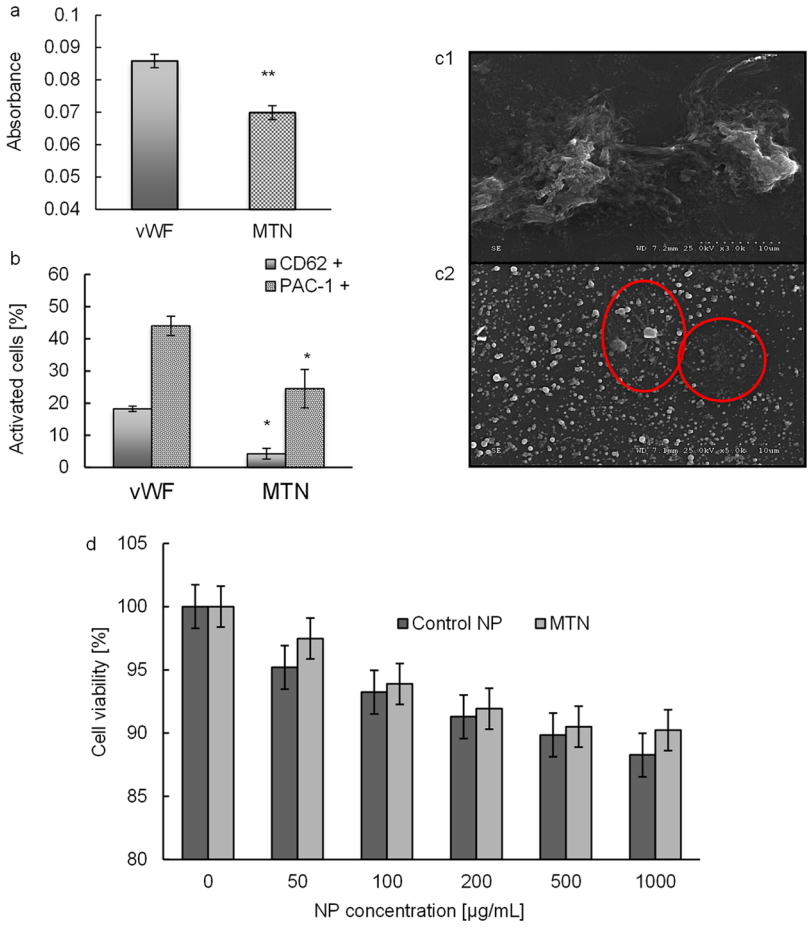

Figure 3. Compatibilities of MTNs. (a) Evaluation of platelet adhesion on vWf and MTN/vWF surfaces *via* LDH assays (at 490 nm). (b) Flow cytometry analysis of platelet activation after incubating with two different substrate coatings by the expression of CD62(+) and PAC-1. * represents $p < 0.05$ *vs* vWF. (c1) SEM image of platelet adhering on the vWF surface. A severe aggregation was observed. (c2) Platelet adhering on MTN-coated vWF surface. Fewer platelets (circled) remained and less activation reaction was observed. (d) Cytocompatibility study of MTNs compared to control NPs. Both groups possess >90% cell viability up to 1000 μg/mL. $N = 3-5$.

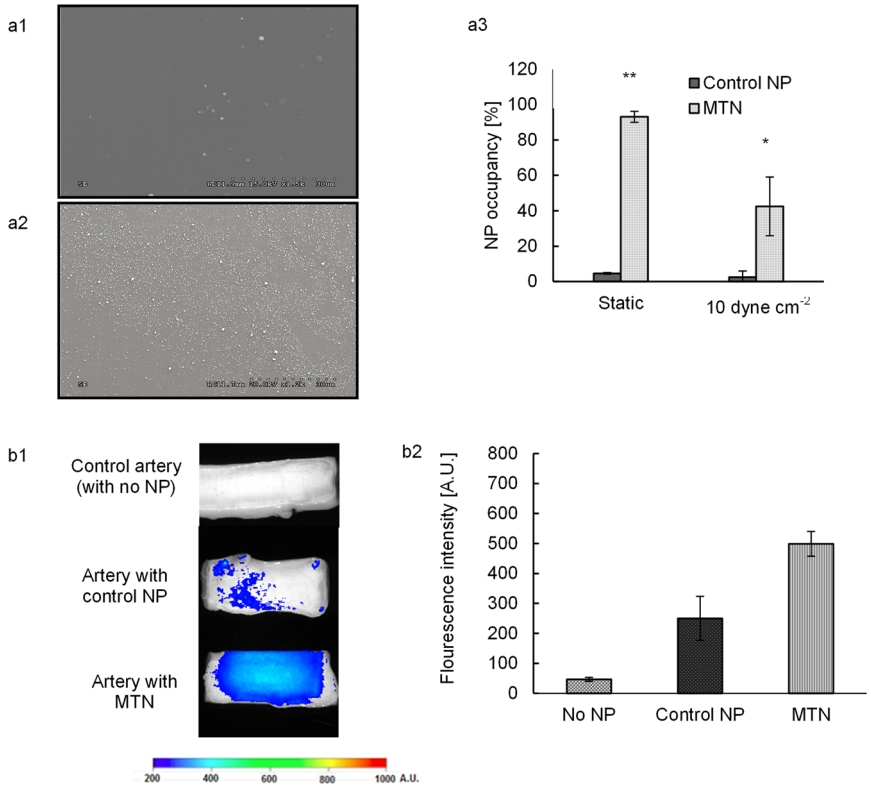

Figure 4. *In vitro* and *ex vivo* targeting efficiency of MTNs. (a1, a2) Scanning electron microscopy images of control NP and MTN adhering on vWF-coated surfaces, respectively, under 10 dyn/cm^2. (a3) Quantification of surface coverage by particle adhesion *via* ImageJ. (b1) Fluorescent images of arteries with lumen injury after incubating with control particles and MTNs. (b2) The fluorescent intensity was determined and compared for three groups: control (no NP), control NP (unconjugated NPs), and MTNs. * represents $p < 0.05$, whereas ** represents $p < 0.01$. $N = 5$.

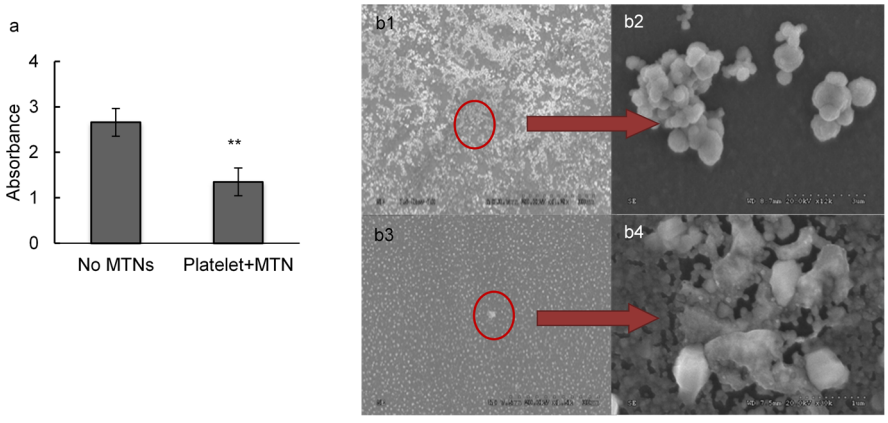

Figure 5. Binding competition of MTNs with platelets. (a) Evaluation of binding competition between platelets and MTNs *via* LDH assay. ** represents $p < 0.01$. (b) SEM image of binding competition studies. SEM images of (b1, b2) platelets incubated on vWF surfaces (scale bars: 30 μm, 3 μm); (b3, b4) platelets and MTNs incubated on vWF surfaces in a platelet competition study (scale bars: 30 μm, 1 μm). $N = 5$.

(Figures 5b1,b2). When MTNs were incubated together with platelets, the vWF-coated surface was covered by mainly MTNs and fewer platelets (Figures 5b3,b4).

***In Vitro* EPC Capturing by MTNs.** Studies were carried to assess the ability of MTNs to attract circulating EPCs. As shown in Figure 6, the rate of EPC adhesion on MTNs was nearly two times as fast as on GPIb-conjugated NPs within the first hour of incubation. Ninety-eight percent of the EPCs adhered on the MTNs at the end of the first hour. On the other hand, the number of cells adhered on GPIb-conjugated NPs appeared to slowly increase and finally reached a similar level in 6 h. After 6 h incubation, cell quantities in both groups reached equilibrium, which might be due to the cell settlement onto the surfaces after seeding for a long time.

Preliminary *in Vivo* Studies of MTNs. The efficacy of MTNs to capture EPCs was evaluated using a rat balloon angioplasty injury model. The accumulation of near-infrared

(NIR)-dye-labeled EPCs at the injury sites was monitored at different time points. Fluorescence emitted from the arteries after animal sacrifice illustrated the capturing of the delivered EPCs by the MTNs at the vascular injury site (Figure 7a). The strongest intensity of the fluorescence was detected 90 min after EPC injection, and it decreased to about 68% after 7 and 21 days.

The extent of angioplasty-induced endothelium injury in the presence or absence of MTNs was also evaluated histologically. Elastin staining was used to identify internal and external elastic lamina (IEL) for evaluating the neointimal hyperplasia of the treated arteries. As shown in Figure 7b, extensive neointima hyperplasia (21st day > seventh day) was observed after the angioplasty procedure in the untreated group (no MTN and EPC injection). In comparison, MTNs and EPC injection suppressed the neointimal hyperplasia after angioplasty (*i.e.*, less intimal area and larger luminal area), as seen in Table 2.

We also studied the endothelium regeneration for injured arteries based on the results of anti-CD31-DAB (which indicates endothelium) IHC staining. Figure 7c compares the outcome between untreated and

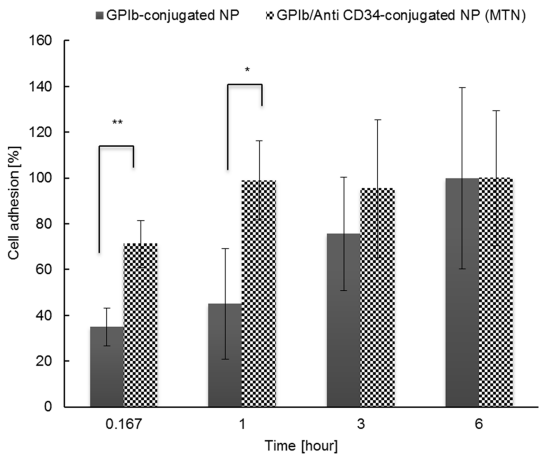

Figure 6. *In vitro* EPC capturing potential of MTNs. The number of EPCs captured by GPIb-conjugated NPs (control) and MTNs was quantified using PicoGreen DNA assays. * represents $p < 0.05$. $N = 3$.

TABLE 2. Histopathological and Angiographic Characteristics of Rat Arteries after Balloon Angioplasty Injury with and without MTN Treatment[a]

	7 days		21 days	
	not treated	treated with MTNs	not treated	treated with MTNs
vessel area, μm^2	53.35×10^4	58.34×10^4	74.88×10^4	56.87×10^4
IEL area, μm^2	35.69×10^4	45.48×10^4	598.73×10^4	37.68×10^4
luminal area, μm^2	28.47×10^4	45.48×10^4	36.12×10^4	30.07×10^4
intimal area, μm^2	7.22×10^4	0.17×10^4	23.60×10^4	7.61×10^4
intimal hyperplasia index	0.1381	0.0025	0.3065	0.1308

[a] Controls are arterial samples without balloon angioplasty injury.

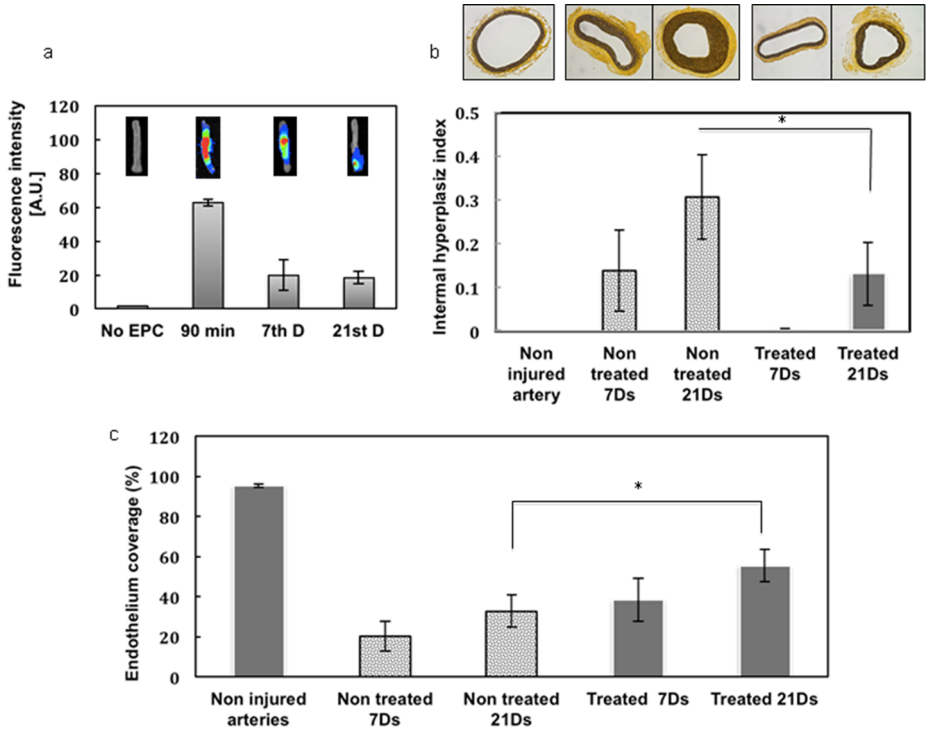

Figure 7. Preliminary *in vivo* evaluation studies of MTNs. (a) Fluorescent emission detected before EPC injection, 1 h after injection (90 min), on the seventh day, and on the 21st day. Fluorescent images of vessel on the upper right are organized sequentially based on time points. (b) Effects of MTNs on suppressing the intimal hyperplasia based on elastin staining images and intimal hyperplasia index. (c) Re-endothelialization of injured arteries untreated and treated with MTNs after 7 and 21 days. * represents $p < 0.05$. $N = 10$.

treated groups after 7 and 21 days. In the untreated specimens, the arterial lumen was covered with an increased endothelial cell number over time, and this phenomenon was significantly enhanced when MTNs were delivered. Equally important, there was a ~60% increase compared to that of the control group in the degree of re-endothelialization after 21 days when the animals were treated with MTNs.

DISCUSSION

Here we report the development of novel MTNs, which combines the advantages of nanotechnology and tissue engineered scaffolding, for treating angioplasty-induced vascular injury. We postulate that by modifying nanoparticle surfaces with both GPIb and anti-CD34 antibodies, the resulting nanoparticle system can perform four major simultaneous functionalities. First, to mimic activated platelets, our nanoparticles were conjugated with platelet GPIb, a region of sulfated tyrosines to appear as main recognition epitopes on platelets for vWF binding.[17] By linking GPIb on the surface, nanoparticles mimic platelet-binding behavior to accumulate at the site of injured vessels especially under high shear rates, thus enabling MTN targeting especially onto the injured arteries. Second, to capture circulating CD34(+) EPC, MTNs were conjugated with anti-CD34 antibody. With antibody on the surface, our results have revealed that MTNs are also capable of capturing EPCs at the injured site, which indirectly reduce platelet adhesion and directly promote endothelium regeneration *in situ*. Third, biodegradable functional MTNs locally delivered to the vascular injury can act as a temporary scaffold that allows for EPC-mediated healthy endothelium formation. In addition, the MTN layer can also act as a temporary barrier to prevent platelet adhesion on the injured site, inhibit smooth muscle cell migration and proliferation, and promote complete regeneration of endothelium. Finally, the MTNs can also serve as payload carriers for various compounds such as growth factors. Through controlled release of the desired compound, this system can provide an optimized environment for EPC proliferation and differentiation, thereby increasing the effectiveness of endothelium regeneration.

UPE, a novel polymer developed in our group for tissue engineering applications,[12] was utilized for particle fabrication due to its demonstrated biodegradability,[18,19] cyto/tissue compatibility, hemocompatibility, and rich functional group for conjugation of biomolecules. The excellent hemocompatibility and cytocompatibility of UPE polymers are advantageous for their use in blood-contacting applications.[12,18,20] Similar to the previous studies demonstrating the hemocompatibility of UPE films and scaffolds,[13] our results of UPE nanoparticles also show hemocompatibility in terms of less platelet adhesion and activation. Biologically, platelet activation can be followed by expression of CD62(+) and PAC-1.[21] Results from SEM, LDH assays, and flow cytometry studies showed less platelet adhesion and activation on substrates after coating of vWF surfaces with MTNs. In addition to hemocompatibility, we also found that MTNs have no apparent toxicity to HAECs up to 1000 μg/mL. These results indicate that MTNs are hemocompatible and noncytotoxic and, thereby, could be used as nanoscaffolds for endothelium regeneration *in situ*.

One of the major motivations of this research is to reduce the complications associated with angioplasty/stenting procedures, such as platelet deposition and activation onto the injured arterial wall. Our nanoparticle scaffold system was designed to mimic the behavior of platelet binding to injured/damaged endothelium *via* the affinity of GPIb to vWF/P-selectin after cardiovascular interventions. Thus, these nanoscaffolds would have the potential to compete with platelets to bind onto the injured arterial wall. In support of this assumption, our results have shown a competitive binding of MTNs at vascular wounds presented as vWF surfaces. It is known that following platelet adhesion and aggregation at the wound site, cytokines are secreted, which activates the cascade of early and late thrombotic complications in patients implanted with coronary stents, including DES.[22] Antiplatelet therapies, although effective, require long-term continuous administration.[23] Different from direct drug administration and DES, our approach is to actively suppress platelet adhesion by blocking platelet adhesion onto vWF/P-selectin using nanoscaffolds localized onto the wound site while simultaneously recruiting EPCs for endothelial regeneration. Inspiringly, our results have shown significant achievements in both targeting the injured arterial wall and homing EPCs onto this site. This might not only increase therapeutic efficacy but also reduce the risk of late thrombosis and restenosis that are often observed after angioplasty/stenting procedures. Other groups have also applied nanoparticles for antithrombosis/antirestenosis treatments. For example, Siddhartha Shrivastava *et al.* delivered nanosilver systemically for antiplatelet purposes and found that these particles accumulated within platelet granules, interfering with interplatelet proximity and reducing their integrin-mediated activation.[24] However, cell, tissue, and organ toxicity might be a concern with repeated treatment of silver nanoparticles. On the other hand, our biodegradable MTN system does not have such limitation, as our materials would be degraded and could be used for a long-term and repeated treatment. In our previous studies, long-term *in vivo* evaluation of the cross-linked UPE scaffolds implanted subcutaneously in Sprague–Dawley rats for 8 and 24 weeks demonstrated that the material was degraded over time and there was no significant chronic inflammation or tissue necrosis in all tested animals.[18] *In vitro* and *in vivo* studies of another urethane-doped citrate-based biodegradable photoluminescent elastomer also show the excellent

cytocompatibility.[19] These studies suggest that the UPE MTN system may not cause a systemic toxicity and inflammation effect, which will be determined extensively in future work.

Polymeric particles, such as polylactic-*co*-glycolic acid (PLGA) nanoparticles, have been extensively developed and used as carriers of therapeutic reagents to treat cardiovascular diseases. For instance, Alexandre C. Zago *et al*. locally delivered sirolimus nanoparticles after PTCA to treat in-stent restenosis in a swine model, which reduced 50% of luminal volume loss and neointimal volume gain.[25] Song C. *et al*. also studied the efficiency of restenosis suppression by allowing cells to take up an antiproliferative agent loaded PLGA nanoparticle.[26] Positive results presented by current research certainly support the feasibility of nanoparticles for drug delivery applications. However, the duration and efficiency of particle retention at the target site under physiological flow conditions might be a limitation. With targeting ligands mimicking the binding of platelets onto the injured arterial wall under blood flow, the localization and retention of our MTNs were substantially enhanced and prolonged when compared to control particles in both *in vitro* and preliminary *in vivo* studies. These exciting observations support that a ligand−receptor targeting strategy can be used to overcome current obstacles. Our study might be the first to investigate the use of nanoparticles serving as multifunctional nanoscaffolds for endothelium regeneration.

Another important aspect of MTN functionality is the capacity of "EPC capturing". It is well understood that anti-CD34 antibodies can be used to recruit endothelial progenitor cells in the circulation.[27,28] Clinical studies on "EPC fishing stents" positively supported the feasibility of applying this antibody against CD34 expressed on EPC surfaces.[29] However, EPCs have to compete with many different cells, especially blood cells and smooth muscle cells (SMCs), *in vivo* on adhesion and proliferation on these implant surfaces.[30] In addition, owing to low selectivity of the anti-CD34 antibody to EPCs, inflammatory/hematopoietic cells were also attracted to the stents.[31] So far no single marker is both highly selective and specific to EPCs. Yet Mario Peichev *et al*. utilized the combination of two markers, AC133 and VEGFR-2, and their results indicate that the accuracy for EPC labeling and identification can be enhanced.[32] In our group, several EPC binding molecules, including anti-CD34 antibodies,[33] anti-VEGFR2 antibodies,[34] laminin-derived peptides YIGSR,[35] phage display-selected peptides TPSLEQRTVYAK,[36] and DNA aptamers,[37] are also tested to filter out the best ligand/antibody combination for EPC capturing in parallel. For "a-proof-of-concept" purpose, anti-CD34 antibody was used in the current experiments. Our *in vitro* results in cell capturing showed a faster adhesion of EPCs when substrates were precoated with MTNs. Furthermore, the presence of EPCs at the vascular injury site in rodent animals also strongly supports the targeting and "EPC capturing" ability of MTNs. These results indicate that MTNs could be used for recruiting EPCs at the injured arterial wall and facilitating endothelium regeneration *in situ*.

Our preliminary *in vivo* studies showed that the group of rodent models treated with MTNs had significantly reduced neointimal formation and enhanced endothelium regeneration. Previous studies have found that the development of early neointima (1 day to 1 month) is due to the SMC proliferation-mediated expansion and deposition of platelets,[38] which released cytokines to up-regulate inflammation activities and promote the dedifferentiation of mature medial smooth muscle cells to a proliferative phenotype.[39] The competitive binding of MTNs onto the injured arterial wall might suppress many platelet-mediated reactions and subsequent SMC responses, therefore successfully decreasing neointimal formation as observed in our animal studies. Additionally, MTNs promoted a more rapid reconstruction of endothelium by locally capturing EPCs and further supporting their adhesion. The nanoscaled MTN surfaces could also be one of the factors stimulating tissue regeneration, as cells are known to adhere effectively onto the micro/nanotopography surfaces.[40,41] After 21 days, our results presented a 60% increase of endothelium regeneration and 53% decrease in neointimal volume gain. These results support that MTNs may be used as a new treatment for angioplasty-induced endothelium injury.

Despite these exciting findings, substantial work is needed on refining the MTN design. For example, the optimal MTN size on endothelium regeneration has yet to be determined. Particle diameters affect the efficiency of particle retention onto the arterial wall as well as control the circulation half-life of particles in the body. It is known that particle sizes below 300 nm tend to be internalized by cells *via* either nonspecific pinocytosis or receptor-mediated endocytosis pathways, whereas particles about 500 nm or larger tend to stay on the cell membrane.[42−44] In addition, particles with a size larger than 300 nm in diameter are often accumulated in the liver, spleen, and lung, making them unavailable at the arterial wall when they are delivered systemically.[45] In this research, nanoparticles have been formulated and used due to many of their advantages in vascular delivery, including ease of local delivery *via* infusion catheters, minimal inflammation, the lessened risk of arterial occlusion, and avoidance of clearance/phagocytosis by the reticuloendothelial system.[45−47] However, microparticles are known to provide more sustained drug release and higher stability and are better for cardiovascular drug delivery applications.[48−51] Future studies will be performed to investigate the effects of different particle sizes *via* catheter infusion delivery for endothelial regeneration

in situ. In addition, the influence of localized released growth factors on endothelium regeneration should be investigated. Better mitotic effects on ECs and greater blood vessel regeneration have been observed when nanoparticles were used to provide the localized release of various growth factors such as VEGF, bFGF, and PDGF.[52,53] Future work will also involve the use of growth factors including VEGF and bFGF to facilitate endothelium regeneration.

CONCLUSIONS

We have developed UPE-based MTNs as a novel nanoscaffolding device to regenerate endothelium *in situ*. This nanoscaffold not only binds to the injured endothelium and/or subendothelium specifically to suppress local reactions regulated by platelet aggregation and activation, but also recruits and supports circulating EPCs for *in situ* endothelium regeneration. Our *in vitro* and *in vivo* results positively supported our hypothesis that MTNs can perform in a site-specific targeting manner by accumulating at the injured endothelium and subendothelium and provide an active mechanism for tissue repair. We believe, under the nanotechnology and tissue-engineering concepts, our multifunctional nanoparticle scaffold may provide a unique approach to treat angioplasty-induced vascular injury.

MATERIALS AND METHODS

Materials. Poly(vinyl alcohol) (PVA), 2-(*N*-morpholino)-ethanesulfonic acid (MES), 1-ethyl(dimethylaminopropyl) carbodiimide, *N*-hydroxysuccinimide (NHS), NIR-797 fluorescent dye, Histopaque-1077, and other chemicals (unless specified) were purchased from Sigma-Aldrich (St. Louis, MO, USA). Recombinant Human GPIb-α was received from R & D System (Minneapolis, MN, USA). Anti-human CD34 antibody was obtained from BD Bioscience (San Jose, CA, USA). Human aortic endothelial cells were purchased from Invitrogen Life Technologies (Grand Island, NY, USA).

Fabrication and Characterization of MTNs. UPE was synthesized in our laboratory as described earlier.[13] UPE NPs were fabricated using a precipitation technique as previously described.[54] In brief, 5 mL of UPE polymer solution (1% w/v in 1,4-dioxane) was added dropwise into a PVA solution (0.1% w/v in deionized water) under constant stirring. After the particle formation, the particle suspension was dialyzed with a 6000−8000 MWCO dialysis tube for 6 h and collected with lyophilization. To formulate MTNs, GPIb and anti-CD34 antibodies were conjugated to the surface of UPE NPs *via* carbodiimide chemistry as previously described.[55] In brief, 15 mg of NHS was added to the UPE NP suspension (10 mg/mL in 0.1 M MES) to activate the carboxyl groups of the NPs. After washing off unreacted materials, 50 μg of GPIb and anti-CD34 antibodies were added into the particle suspension and incubated for 3 h with continuous shaking at room temperature. At the end of the reaction, NPs were washed *via* dialysis and ultracentrifugation. After lyophilization, the MTNs (dual-ligand-conjugated NPs) were collected.

The particle sizes, size distribution, and surface potential were measured *via* the dynamic light scattering (DLS) method using a ZetaPALS zeta potential analyzer (Brookhaven Instruments Inc., Holtsville, NY, USA). Scanning electron microscopy (Hitachi S-3000N variable pressure, Hitachi, Pleasanton, CA, USA) and transmission electron microscopy (Tecnai G2 Spirit 120 kV, FEI, Hillsboro, OR, USA) were also used to measure the size and observe the morphology of the NPs.

Bovine serum albumin (BSA) was used as a model protein to evaluate the drug delivery property of the NPs. BSA-loaded NPs were formulated similarly to that mentioned above with a slight modification of adding the BSA solution (20 mg of BSA in 200 μL of deionized water) into the polymer solution for NP fabrication. BSA loading efficiency in the NPs was calculated indirectly by subtracting the amount of BSA not loaded in the NPs from the total amount of used BSA. To study the protein releasing profile from the UPE NPs, BSA-loaded NPs were resuspended in phosphate buffered saline (PBS) and incubated at 37 °C. At different time points (0, 1, 4, 7, 11, 16, 21, and 30 days from incubation), the supernatant was collected and the released BSA was quantified using the BCA protein assays. The cumulative percent BSA release was then plotted against the incubation time.

To study the NP degradation, UPE NPs were incubated in PBS at 37 °C. At predetermined time points, the particle size was measured using DLS. The particle weight was also recorded after lyophilization. The particle diameter reduction percentage was calculated as (initial average particle diameter − measured average particle diameter after incubation)/initial average particle diameter.

***In Vitro* Hemocompatibility and Cytocompatibility of MTNs.** Hemocompatibility of MTNs was evaluated by studying platelet adhesion, activation, and blood clotting on MTNs.[12] vWF (5 μg/mL) was coated on glass slides to mimic the injured arterial wall surface (with overexpressed vWF). MTNs (400 μg/mL) were attached on the vWF surfaces as previously described.[55] After preparing the testing surfaces (vWF or MTN), platelet-rich plasma was added on top and incubated for 1 h. Adhered platelets were quantified using LDH assays (Promega Corporation, Madison, WI, USA) following the manufacturer's instructions. Adhered platelets were also observed using SEM. Platelet activation was further evaluated by detecting P-selectin (CD-62p) and PAC-1 expression on the exposed platelets using flow cytometry (BD Calibur) as previously described.[2]

To study the cytotoxicity of the MTNs, HAECs grown in 96-well plates were allowed to reach 80% confluence and then incubated with MTNs or unmodified UPE NPs (control NPs) for 24 h at 37 °C. The concentrations of the NPs studied were 0, 50, 100, 200, 500, and 1000 μg/mL. After incubation, cell cytotoxicity was measured using MTS assays (Promega Corporation, Madison, WI, USA) following the manufacturer's instructions.

MTN's Targeting to vWF *in Vitro* and Injured Blood Vessel *ex Vivo*. To study the NP targeting in static conditions, suspensions (200 μg/mL) of MTNs or unmodified UPE NPs (control group) were incubated on vWF-coated glass sides for 1 h. To determine the NP targeting in the flow condition, NP suspensions were flown over the vWF-coated glass sides at 10 dyn/cm^2 using a parallel flow system.[16] After a 30 min flow, the glass slides were gently rinsed with PBS to remove loosely bound NPs and examined with SEM. The images were analyzed using ImageJ software to calculate the NP coverage on the vWF substrate.

In the *ex vivo* NP targeting study, near-infrared dye (NIR-797)-loaded MTNs were incubated on the luminal surface of the fresh porcine aorta after scraping off the endothelium. After an hour of incubation, the arteries were rinsed to remove loosely bound NPs. A Kodak *in vivo* FX imaging system (Carestream, Rochester, NY, USA) was employed to observe the NPs bound on the arterial wall and measure the fluorescent intensity of the NPs adhered on the arteries.

Binding Competition of MTNs and Platelets on vWF. In order to simulate the platelet numbers in platelet-rich plasma (PRP) (2×10^8/ mL), 16.8 μg/mL of MTN (average particle size 400 nm) was used in this study based on the calculation described previously.[55,56] The MTN suspension (200 μL) was mixed with 200 μL of PRP and added on top of vWF-coated glass slides and incubated for 1 h. In the other group, PRP (200 μL) was incubated on vWF surfaces for the same period of time. After incubation, the slides were gently rinsed, and LDH assays were used to quantify the platelets adhered as described above. In parallel, substrates were also prepared for SEM observation.

***In Vitro* EPC Capturing by MTNs.** EPCs were isolated from blood using Histopaue-1077 (Sigma-Aldrich) following the manufacturer's procedures. In brief, the mononuclear fraction was collected after density gradient centrifugation. Cells were cultured using the endothelial basal medium-2 supplemented with EGM-2 SingleQuots (Lonza) until enough cells were achieved. To evaluate the EPC-capturing functionality, MTNs (GPIb/anti-CD34 antibodies conjugated) or GPIb-conjugated (one ligand) UPE NPs were incubated on vWF-coated surfaces as described above. To study EPC capturing, EPCs (10^5 cells/mL) were incubated on the substrates for 10 min, 1 h, 3 h, and 6 h under constant agitation at 37 °C. After gently washing, immobilized EPCs were lysed and quantified with PicoGreen DNA assays (Life Technologies, Carlsbad, CA, USA) following the manufacturer's instructions.

***In Vivo* Animal Study.** Animal experiments were conducted according to the animal welfare and IACUC-approved protocols from the University of Texas at Arlington. Sprague−Dawley male rats (one year old) approximately 300−500 g in weight were used in a balloon angioplasty injury model. Under anesthesia, rat carotid arteries were first identified and 2F angioplasty balloon catheters were carefully inserted from the external carotid artery into the common carotid artery. Vascular injuries were created by repeated inflation of the balloon at 8 atm. Next, MTNs (400 μg/mL) were infused into the injured artery segment as previously described.[57] Subsequently, rat EPCs were isolated and labeled with NIR dyes using procedures described earlier[58−60] and were injected to the artery to determine whether the MTNs could be used for EPC capturing *in vivo*. Wounds were closed and the animals were kept for 90 min, 7 days, and 21 days before being sacrificed. For evaluation, arteries were collected and stained by hematoxylin and eosin (H&E), as well as elastin staining, to determine the vascular stenosis (*i.e.*, neointima hyperplasia). Moreover, immunohistochemical staining with anti-CD31 antibodies was used to identify the regenerated endothelial cells on the vessel. Recovery of injured vessels was calculated as the percentage of luminal surface covered by endothelium.

Statistical Analysis. Results were analyzed statistically using a two-way ANOVA (StatView 5.0 software, SAS Institute, Cary, NC, USA) with $p < 0.05$ between samples considered as a significant difference. *Post hoc* comparisons were made using the Fisher's least significant differences (LSD). All the results are given as mean ± SD ($N = 3-10$).

Conflict of Interest: The authors declare no competing financial interest.

Acknowledgment. This work was supported in part by the National Heart, Lung, and Blood Institute (NHLBI) of the National Institutes of Health (NIH) under the award grant numbers NHLBI HL 118498 (to K.N. and J.Y.) and NIH awards (EB 012575 and CA 182670 to J.Y.), NSF awards (DMR 1313553 and CMMI 1266116 to J.Y.), and AHA Grant-in-Aid awards (13GRNT17330010 to K.N. and 10GRNT4580013 to L.T.). The content is solely the responsibility of the authors and does not necessarily represent the official views of the NHLBI, NIH, NSF, or AHA. The authors would also like to thank Dr. John M. Shelton, a senior research scientist at the UT Southwestern Molecular Pathology Core, for his help with vessel sectioning, staining, and analysis, and Ms. Alicia J. Sisemore for her help with manuscript editing.

REFERENCES AND NOTES

1. Fischman, D. L.; Leon, M. B.; Baim, D. S.; Schatz, R. A.; Savage, M. P.; Penn, I.; Detre, K.; Veltri, L.; Ricci, D.; Nobuyoshi, M. A Randomized Comparison of Coronary-Stent Placement and Balloon Angioplasty in the Treatment of Coronary Artery Disease. Stent Restenosis Study Investigators. *N. Engl. J. Med.* **1994**, *331*, 496–501.
2. Xu, H.; Deshmukh, R.; Timmons, R.; Nguyen, K. T. Enhanced Endothelialization on Surface Modified Poly(L-Lactic Acid) Substrates. *Tissue Eng. Part A* **2011**, *17*, 865–876.
3. Becker, B. F.; Heindl, B.; Kupatt, C.; Zahler, S. Endothelial Function and Hemostasis. *Z. Kardiol.* **2000**, *89*, 160–167.
4. Zolpi, E.; Filipetto, C.; Bertipaglia, B.; Taiani, J.; Gasparotto, L.; Chiavegato, A.; Gamba, P.; Sartore, S. Role of Platelet Activation in Catheter-Induced Vascular Wall Injury. *J. Endovasc. Ther.* **2004**, *11*, 196–210.
5. McFadden, E. P.; Stabile, E.; Regar, E.; Cheneau, E.; Ong, A. T.; Kinnaird, T.; Suddath, W. O.; Weissman, N. J.; Torguson, R.; Kent, K. M. Late Thrombosis in Drug-Eluting Coronary Stents after Discontinuation of Antiplatelet Therapy. *Lancet* **2004**, *364*, 1519–1521.
6. Deglau, T. E.; Maul, T. M.; Villanueva, F. S.; Wagner, W. R. In Vivo PEG Modification of Vascular Surfaces for Targeted Delivery. *J. Vasc. Surg.* **2012**, *55*, 1087–1095.
7. Rossi, M. L.; Zavalloni, D.; Gasparini, G. L.; Mango, R.; Belli, G.; Presbitero, P. The First Report of Late Stent Thrombosis Leading to Acute Myocardial Infarction in Patient Receiving the New Endothelial Progenitor Cell Capture Stent. *Int. J. Cardiol.* **2010**, *141*, e20–22.
8. Asahara, T.; Murohara, T.; Sullivan, A.; Silver, M.; van der Zee, R.; Li, T.; Witzenbichler, B.; Schatteman, G.; Isner, J. M. Isolation of Putative Progenitor Endothelial Cells for Angiogenesis. *Science* **1997**, *275*, 964–967.
9. Zampetaki, A.; Kirton, J. P.; Xu, Q. Vascular Repair by Endothelial Progenitor Cells. *Cardiovasc. Res.* **2008**, *78*, 413–421.
10. Co, M.; Tay, E.; Lee, C. H.; Poh, K. K.; Low, A.; Lim, J.; Lim, I. H.; Lim, Y. T.; Tan, H. C. Use of Endothelial Progenitor Cell Capture Stent (Genous Bio-Engineered R Stent) during Primary Percutaneous Coronary Intervention in Acute Myocardial Infarction: Intermediate- to Long-Term Clinical Follow-Up. *Am. Heart J.* **2008**, *155*, 128–132.
11. Ho, H. H.; Chow, W. H.; Ko, L. Y.; Jim, M. H. Successful Use of Endothelial Progenitor Cell Capture Stent for Treatment of Left Main Coronary Artery Disease before Non-Cardiac Surgery for Abdominal Aortic Aneurysm. *Int. J. Cardiol.* **2010**, *143*, e27–29.
12. Dey, J.; Xu, H.; Nguyen, K. T.; Yang, J. Crosslinked Urethane Doped Polyester Biphasic Scaffolds: Potential for in Vivo Vascular Tissue Engineering. *J. Biomed. Mater. Res. A* **2010**, *95*, 361–370.
13. Dey, J.; Xu, H.; Shen, J.; Thevenot, P.; Gondi, S. R.; Nguyen, K. T.; Sumerlin, B. S.; Tang, L.; Yang, J. Development of Biodegradable Crosslinked Urethane-Doped Polyester Elastomers. *Biomaterials* **2008**, *29*, 4637–4649.
14. Firbas, C.; Siller-Matula, J. M.; Jilma, B. Targeting Von Willebrand Factor and Platelet Glycoprotein Ib Receptor. *Expert Rev. Cardiovasc. Ther.* **2010**, *8*, 1689–1701.
15. Aoki, J.; Serruys, P. W.; van Beusekom, H.; Ong, A. T.; McFadden, E. P.; Sianos, G.; van der Giessen, W. J.; Regar, E.; de Feyter, P. J.; Davis, H. R. Endothelial Progenitor Cell Capture by Stents Coated with Antibody against Cd34: The Healing-Fim (Healthy Endothelial Accelerated Lining Inhibits Neointimal Growth-First in Man) Registry. *J. Am. Coll. Cardiol.* **2005**, *45*, 1574–1579.
16. Kona, S.; Dong, J. F.; Liu, Y.; Tan, J.; Nguyen, K. T. Biodegradable Nanoparticles Mimicking Platelet Binding as a Targeted and Controlled Drug Delivery System. *Int. J. Pharm.* **2012**, *423*, 516–524.
17. Hagay, Y.; Lahav, J.; Levanon, A.; Varon, D.; Brill, A.; Panet, A. Molecular Characterization of a Human Monoclonal Antibody That Interacts with a Sulfated Tyrosine-Containing Epitope of the Gpib Receptor and Inhibits Platelet Functions. *Mol. Immunol.* **2006**, *43*, 443–453.
18. Dey, J.; Tran, R. T.; Shen, J.; Tang, L.; Yang, J. Development and Long-Term in Vivo Evaluation of a Biodegradable Urethane-Doped Polyester Elastomer. *Macromol. Mater. Eng.* **2011**, *296*, 1149–1157.
19. Zhang, Y.; Tran, R. T.; Qattan, I. S.; Tsai, Y. T.; Tang, L.; Liu, C.; Yang, J. Fluorescence Imaging Enabled Urethane-Doped Citrate-Based Biodegradable Elastomers. *Biomaterials* **2013**, *34*, 4048–4056.
20. Tran, R. T.; Zhang, Y.; Gyawali, D.; Yang, J. Recent Developments on Citric Acid Derived Biodegradable Elastomers. *Recent Pat. Biomed. Eng.* **2009**, *2*, 216–227.
21. Johansson, M. W.; Han, S. T.; Gunderson, K. A.; Busse, W. W.; Jarjour, N. N.; Mosher, D. F. Platelet Activation, P-Selectin,

and Eosinophil Beta1-Integrin Activation in Asthma. *Am. J. Respir. Crit. Care Med.* **2012**, *185*, 498–507.
22. Jin, C.; Lu, L.; Zhu, Z. B.; Zhang, R. Y.; Zhang, Q.; Du, R.; Ding, F. H.; Chen, Q. J.; Shen, W. F. Increased Serum vWF and Svcam-1 Levels Are Associated with Late or Very Late Angiographic Stent Thrombosis after Sirolimus-Eluting Stent Implantation. *Coron Artery Dis.* **2010**, *21*, 273–277.
23. Kurz, D. J.; Eberli, F. R. Medical Therapy of Coronary Artery Disease after Percutaneous Intervention. *Curr. Opin. Pharmacol.* **2013**, *13*, 287–293.
24. Shrivastava, S.; Bera, T.; Singh, S. K.; Singh, G.; Ramachandrarao, P.; Dash, D. Characterization of Antiplatelet Properties of Silver Nanoparticles. *ACS Nano* **2009**, *3*, 1357–1364.
25. Zago, A. C.; Raudales, J. C.; Attizzani, G.; Matte, B. S.; Yamamoto, G. I.; Balvedi, J. A.; Nascimento, L.; Kosachenco, B. G.; Centeno, P. R.; Zago, A. J. Local Delivery of Sirolimus Nanoparticles for the Treatment of in-Stent Restenosis. *Catheter Cardiovasc. Interv.* **2013**, *81*, e124–129.
26. Song, C.; Labhasetwar, V.; Cui, X.; Underwood, T.; Levy, R. J. Arterial Uptake of Biodegradable Nanoparticles for Intravascular Local Drug Delivery: Results with an Acute Dog Model. *J. Controlled Release* **1998**, *54*, 201–211.
27. Eggermann, J.; Kliche, S.; Jarmy, G.; Hoffmann, K.; Mayr-Beyrle, U.; Debatin, K. M.; Waltenberger, J.; Beltinger, C. Endothelial Progenitor Cell Culture and Differentiation in Vitro: A Methodological Comparison Using Human Umbilical Cord Blood. *Cardiovasc. Res.* **2003**, *58*, 478–486.
28. Hristov, M.; Erl, W.; Weber, P. C. Endothelial Progenitor Cells: Mobilization, Differentiation, and Homing. *Arterioscler. Thromb. Vasc. Biol.* **2003**, *23*, 1185–1189.
29. Larsen, K.; Cheng, C.; Tempel, D.; Parker, S.; Yazdani, S.; den Dekker, W. K.; Houtgraaf, J. H.; de Jong, R.; Swager-ten Hoor, S.; Ligtenberg, E. Capture of Circulatory Endothelial Progenitor Cells and Accelerated Re-endothelialization of a Bio-Engineered Stent in Human ex Vivo Shunt and Rabbit Denudation Model. *Eur. Heart J.* **2012**, *33*, 120–128.
30. Wei, Y.; Ji, Y.; Xiao, L. L.; Lin, Q. K.; Xu, J. P.; Ren, K. F.; Ji, J. Surface Engineering of Cardiovascular Stent with Endothelial Cell Selectivity for in Vivo Re-endothelialisation. *Biomaterials* **2013**, *34*, 2588–2599.
31. Wendel, H. P.; Avci-Adali, M.; Ziemer, G. Endothelial Progenitor Cell Capture Stents—Hype or Hope?. *Int. J. Cardiol.* **2010**, *145*, 115–117.
32. Peichev, M.; Naiyer, A. J.; Pereira, D.; Zhu, Z.; Lane, W. J.; Williams, M.; Oz, M. C.; Hicklin, D. J.; Witte, L.; Moore, M. A. Expression of Vegfr-2 and Ac133 by Circulating Human Cd34(+) Cells Identifies a Population of Functional Endothelial Precursors. *Blood* **2000**, *95*, 952–958.
33. Rotmans, J. I.; Heyligers, J. M.; Verhagen, H. J.; Velema, E.; Nagtegaal, M. M.; de Kleijn, D. P.; de Groot, F. G.; Stroes, E. S.; Pasterkamp, G. In Vivo Cell Seeding with Anti-Cd34 Antibodies Successfully Accelerates Endothelialization but Stimulates Intimal Hyperplasia in Porcine Arteriovenous Expanded Polytetrafluoroethylene Grafts. *Circulation* **2005**, *112*, 12–18.
34. Markway, B. D.; McCarty, O. J.; Marzec, U. M.; Courtman, D. W.; Hanson, S. R.; Hinds, M. T. Capture of Flowing Endothelial Cells Using Surface-Immobilized Anti-Kinase Insert Domain Receptor Antibody. *Tissue Eng. Part C Methods* **2008**, *14*, 97–105.
35. Taite, L. J.; Yang, P.; Jun, H. W.; West, J. L. Nitric Oxide-Releasing Polyurethane-PEG Copolymer Containing the Yigsr Peptide Promotes Endothelialization with Decreased Platelet Adhesion. *J. Biomed. Mater. Res. B: Appl. Biomater.* **2008**, *84*, 108–116.
36. Veleva, A. N.; Heath, D. E.; Cooper, S. L.; Patterson, C. Selective Endothelial Cell Attachment to Peptide-Modified Terpolymers. *Biomaterials* **2008**, *29*, 3656–3661.
37. Hoffmann, J.; Paul, A.; Harwardt, M.; Groll, J.; Reeswinkel, T.; Klee, D.; Moeller, M.; Fischer, H.; Walker, T.; Greiner, T. Immobilized DNA Aptamers Used as Potent Attractors for Porcine Endothelial Precursor Cells. *J. Biomed. Mater. Res. A* **2008**, *84*, 614–621.
38. Wu, J.; Zhang, C. Neointimal Hyperplasia, Vein Graft Remodeling, and Long-Term Patency. *Am. J. Physiol. Heart Circ. Physiol.* **2009**, *297*, H1194–1195.
39. Jiang, Z.; Tao, M.; Omalley, K. A.; Wang, D.; Ozaki, C. K.; Berceli, S. A. Established Neointimal Hyperplasia in Vein Grafts Expands via TGF-Beta-Mediated Progressive Fibrosis. *Am. J. Physiol. Heart Circ. Physiol.* **2009**, *297*, H1200–1207.
40. Gittens, R. A.; McLachlan, T.; Olivares-Navarrete, R.; Cai, Y.; Berner, S.; Tannenbaum, R.; Schwartz, Z.; Sandhage, K. H.; Boyan, B. D. The Effects of Combined Micron-/Submicron-Scale Surface Roughness and Nanoscale Features on Cell Proliferation and Differentiation. *Biomaterials* **2011**, *32*, 3395–3403.
41. Silva, T. S.; Machado, D. C.; Viezzer, C.; Silva Junior, A. N.; Oliveira, M. G. Effect of Titanium Surface Roughness on Human Bone Marrow Cell Proliferation and Differentiation: An Experimental Study. *Acta Circ. Bras.* **2009**, *24*, 200–205.
42. Oyewumi, M. O.; Kumar, A.; Cui, Z. Nano-Microparticles as Immune Adjuvants: Correlating Particle Sizes and the Resultant Immune Responses. *Expert Rev. Vaccines* **2010**, *9*, 1095–1107.
43. Charoenphol, P.; Huang, R. B.; Eniola-Adefeso, O. Potential Role of Size and Hemodynamics in the Efficacy of Vascular-Targeted Spherical Drug Carriers. *Biomaterials* **2010**, *31*, 1392–1402.
44. Muro, S.; Garnacho, C.; Champion, J. A.; Leferovich, J.; Gajewski, C.; Schuchman, E. H.; Mitragotri, S.; Muzykantov, V. R. Control of Endothelial Targeting and Intracellular Delivery of Therapeutic Enzymes by Modulating the Size and Shape of ICAM1-Targeted Carriers. *Mol. Ther.* **2008**, *16*, 1450–1458.
45. Brito, L.; Amiji, M. Nanoparticulate Carriers for the Treatment of Coronary Restenosis. *Int. J. Nanomed.* **2007**, *2*, 143–161.
46. Sun, D. X.; Liu, Z.; Tan, X. D.; Cui, D. X.; Wang, B. S.; Dai, X. W. Nanoparticle-Mediated Local Delivery of an Antisense TGF-Beta1 Construct Inhibits Intimal Hyperplasia in Autogenous Vein Grafts in Rats. *PLoS One* **2012**, *7*, e41857.
47. Moghimi, S. M.; Hunter, A. C.; Murray, J. C. Nanomedicine: Current Status and Future Prospects. *FASEB J.* **2005**, *19*, 311–330.
48. Kohane, D. S. Microparticles and Nanoparticles for Drug Delivery. *Biotechnol. Bioeng.* **2007**, *96*, 203–209.
49. Charoenphol, P.; Mocherla, S.; Bouis, D.; Namdee, K.; Pinsky, D. J.; Eniola-Adefeso, O. Targeting Therapeutics to the Vascular Wall in Atherosclerosis—Carrier Size Matters. *Atherosclerosis* **2011**, *217*, 364–370.
50. Eniola-Adefeso, O.; Heslinga, M. J.; Porter, T. M. Design of Nanovectors for Therapy and Imaging of Cardiovascular Diseases. *Methodist Debakey Cardiovasc. J.* **2012**, *8*, 13–17.
51. Namdee, K.; Thompson, A. J.; Charoenphol, P.; Eniola-Adefeso, O. Margination Propensity of Vascular-Targeted Spheres from Blood Flow in a Microfluidic Model of Human Microvessels. *Langmuir* **2013**, *29*, 2530–2535.
52. Kolachala, V. L.; Henriquez, O. A.; Shams, S.; Golub, J. S.; Kim, Y. T.; Laroui, H.; Torres-Gonzalez, E.; Brigham, K. L.; Rojas, M.; Bellamkonda, R. V. Slow-Release Nanoparticle-Encapsulated Delivery System for Laryngeal Injection. *Laryngoscope* **2010**, *120*, 988–994.
53. Zhang, H.; Jia, X.; Han, F.; Zhao, J.; Zhao, Y.; Fan, Y.; Yuan, X. Dual-Delivery of VEGF and PDGF by Double-Layered Electrospun Membranes for Blood Vessel Regeneration. *Biomaterials* **2013**, *34*, 2202–2212.
54. Xie, H.; Smith, J. W. Fabrication of PLGA Nanoparticles with a Fluidic Nanoprecipitation System. *J. Nanobiotechnol.* **2010**, *8*, 18.
55. Lin, A.; Sabnis, A.; Kona, S.; Nattama, S.; Patel, H.; Dong, J. F.; Nguyen, K. T. Shear-Regulated Uptake of Nanoparticles by Endothelial Cells and Development of Endothelial-Targeting Nanoparticles. *J. Biomed. Mater. Res. A* **2010**, *93*, 833–842.
56. Goldberg, M.; Langer, R.; Jia, X. Nanostructured Materials for Applications in Drug Delivery and Tissue Engineering. *J. Biomater. Sci. Polym. Ed* **2007**, *18*, 241–268.
57. Tulis, D. A. Rat Carotid Artery Balloon Injury Model. *Methods Mol. Med.* **2007**, *139*, 1–30.
58. Thevenot, P. T.; Nair, A. M.; Shen, J.; Lotfi, P.; Ko, C. Y.; Tang, L. The Effect of Incorporation of SDF-1alpha into PLGA

Scaffolds on Stem Cell Recruitment and the Inflammatory Response. *Biomaterials* **2010**, *31*, 3997–4008.
59. Nair, A. M.; Tsai, Y. T.; Shah, K. M.; Shen, J.; Weng, H.; Zhou, J.; Sun, X.; Saxena, R.; Borrelli, J., Jr.; Tang, L. The Effect of Erythropoietin on Autologous Stem Cell-Mediated Bone Regeneration. *Biomaterials* **2013**, *34*, 7364–7371.
60. Nair, A.; Shen, J.; Lotfi, P.; Ko, C. Y.; Zhang, C. C.; Tang, L. Biomaterial Implants Mediate Autologous Stem Cell Recruitment in Mice. *Acta Biomater.* **2011**, *7*, 3887–3895.